A Robust Nonlinear Control Approach for Tip Position Tracking of Flexible Spacecraft

MARYAM MALEKZADEH
ABOLGHASEM NAGHASH
H. A. TALEBI, Senior Member, IEEE
Amirkabir University of Technology

In this paper, the problem of attitude control of a 3D nonlinear flexible spacecraft is investigated. Two nonlinear controllers are presented. The first controller is based on dynamic inversion, while the second approach is composed of dynamic inversion and μ-synthesis schemes. The extension of dynamic inversion approach to flexible spacecraft is impeded by the nonminimum phase characteristics when the panel tip position is taken as the output of the system. To overcome this problem, the controllers are designed by utilizing the modified output redefinition approach. It is assumed that only three torques in three directions on the hub are used. Actuator saturation is also considered in the design of controllers. To evaluate the performance of the proposed controllers, an extensive number of simulations on a nonlinear model of the spacecraft are performed. The performances of the proposed controllers are compared in terms of nominal performance, robustness to uncertainties, vibration suppression of panel, sensitivity to measurement noise, environment disturbance, and nonlinearity in large maneuvers. Simulation results confirm the ability of the proposed controller in tracking the attitude trajectory while damping the panel vibration. It is also verified that the perturbations, environment disturbances, and measurement errors have only slight effects on the tracking and damping performances.

Manuscript received January 24, 2009; revised July 7 and November 25, 2009; released for publication February 23, 2010.

IEEE Log No. T-AES/47/4/942879.

Refereeing of this contribution was handled by M. Makella.

Authors' address: M. Malekzadeh and A. Naghash, Dept. of Aerospace Engineering, Amirkabir University of Technology, Tehran, Iran, E-mail: (malekzadeh@aut.ac.ir); H. A. Talebi, Dept. of Electrical Engineering, Amirkabir University of Technology, Tehran, Iran.

I. INTRODUCTION

The problem of attitude control of satellites undergoing large angle motion has received a great deal of attention in recent years and several methods have been developed to address this problem. The large-angle maneuvers are characterized by nonlinear dynamics and hence nonlinear control design is often required.

A common method to control space vehicles is to use a linear controller designed for the linear approximation of the nonlinear system around an operating point. This method is largely used because linear systems there are a variety of well-established control techniques and the design can be done in a more systematic way than for nonlinear cases. Nevertheless the linear control techniques work in general only in a small neighborhood of the operating point where the linear approximation is valid.

In the context of nonlinear systems, the feedback linearization seems a viable choice since the nonlinear system is exactly transformed into a linear system (valid for the entire operating region) and only when the linear controller is applied. Therefore the dynamic range of the closed-loop system is increased. However, the classical feedback linearization suffers from the lack of robustness in the presence of uncertainties, disturbances, and noise.

In [1] the problem of attitude recovery of flexible spacecraft with the plate-type appendages using the feedback linearization approach was investigated. The controller ability is shown in the recovery maneuver and panel vibration suppression. However, the performance is only tested for impulse disturbance (thruster effect); it is notable that feedback linearization is robust against impulse disturbance but is very weak against constant disturbances. Although this method achieves good vibration suppression, it does not address the issue of robustness to combined uncertain conditions (several uncertain conditions, i.e., environment disturbance, sensor noise, and uncertain parameters exist together or there is one uncertain condition with larger variations). Moreover the selected controller bound is large as if the actuator saturation has not been considered.

Recently considerable efforts have been made to design robust control systems for simultaneous attitude control and vibration suppression of flexible spacecraft. However most of the works are based on the linear control approach which results in a poor performance for large maneuvers. For instance in [2] an experimental flexible arm serves as a test bed to investigate the efficiency of the μ-synthesis design technique in controlling flexible manipulators. In [3] the active optimal attitude control of a three-axis stabilized spacecraft by flywheels was studied. The corresponding time-varying linear quadratic regulators (LQRs) are designed for the approximate system.

Various nonlinear robust control algorithms have been proposed on rigid spacecraft such as a mixed H_2/H_8 controller incorporating a cerebellar model articulation controller learning method [4], adaptive fuzzy mixed H_2/H_8 [5], adaptive mixed H_2/H_8 [6], LMI [7], and other nonlinear control schemes [8].The neural networks or fuzzy or adaptive methods are employed to approximate the unknown nonlinearities of system dynamics. However, other uncertainties such as sensor noise and environment disturbances have not been considered in these works.

Although nonlinear robust control methods, such as nonlinear H_8 control can be applied to address these issues, solving the associated Hamilton-Jacobi equation is often extremely complicated and the resulting controller is not easy to implement. Consequently, a robust feedback linearization strategy seems promising.

In [9] and [10], adaptive feedback linearizing and inverse optimal adaptive control laws were derived for the trajectory control of the pitch angle. Unmodeled parameters appearing in the inverse feedback linearization control law are estimated using a high gain observer. However other uncertainties such as sensor noise and environment disturbances have not been considered. In [11] a hybrid control scheme with variable structure and an intelligent adaptive control method were used for control of flexible space structures. In [12] an inverse adaptive controller using solar radiation pressure was utilized.

The most common approach to compensate for the nonlinear dynamics of a rigid spacecraft is the so-called inverse dynamics strategy. However, the extension of this approach to flexible spacecraft is impeded by the nonminimum phase characteristics when the panel tip position is taken as the output of the system. To overcome this problem, a new output was defined in [13] so that the zero dynamics related to this output are stable. In [14] the performance of neural network-based controllers is presented for tip position tracking of flexible-link manipulators. The controller was designed by utilizing the modified output redefinition approach. However, this method has never been used for a spacecraft control system.

The objective of this paper is to develop a new approach for robust attitude control and vibration suppression of flexible spacecraft. The attitude control of a 3D flexible spacecraft is addressed using two approaches: dynamic inversion and the composition of dynamic inversion and μ-synthesis. The goal is the attitude control and panel vibration suppression in the absence of damping and actuators on panels.

To overcome the nonminimum phase characteristics of the tip-position output, the controllers are designed by utilizing the modified output redefinition approach. It is well known that the zero dynamics of a flexible spacecraft associated with the panel deflection is unstable. Hence the sum of the attitude angles and a scaling of the tip elastic deformation are chosen as the output. This scale results in stable zero dynamics of the system. Hence in the design of dynamic inversion controller, this summation is considered as the output.

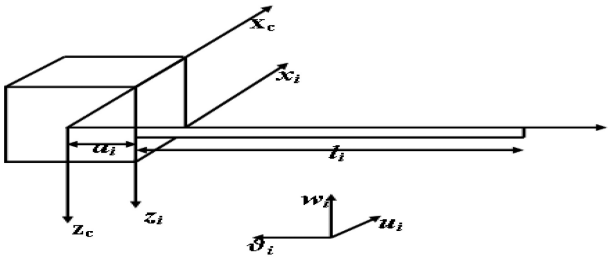

Fig. 1. Flexible spacecraft model.

To account for inexact dynamic cancellation arising in the inner-loop feedback linearization (dynamic inversion) design, the μ-synthesis control law is formulated such that an outer-loop linear controller can be constructed to provide robust stability/performance against such inexact cancellation.

To enforce the position and rate saturation limit, a feedback controller structure is used in the inner loop. Another important issue in designing the μ-synthesis controller is bounding the linear controller term which is different from the bound for the actual control signal u. Hence it is crucial to find an appropriate weighting function for the linear controller. To evaluate the performance of the proposed controllers, a set of simulations are performed on a 3D stabilized flexible spacecraft. It was our intention that the sensors noises, disturbances, and uncertainty be as close as possible to practical situations.

The paper is organized as follows. In Section II, dynamic equations of flexible spacecraft are given. The output redefinition approach is discussed in Section III. The design of two controllers, namely a nonlinear dynamic inversion controller and a composite controller (with inner-loop feedback linearization and outer-loop μ-synthesis) is presented in Sections IV and V, respectively. Section VI demonstrates the computer simulations of the spacecraft attitude tracking and suppression panel vibration. Section VII concludes the paper.

II. FLEXIBLE SPACECRAFT EQUATIONS

The system under investigation consists of a rigid hub and N appendages attached to it. According to Fig. 1, each appendage has linear density (mass per unit length) ρ_i, length l_i, and is attached at a distance a_i from the hub.

The kinetic energy of the system is composed of kinetic energies of the hub, and the appendages. This kinetic energy can be written in the form of

$$T = \tfrac{1}{2}\omega^T I_c \omega + \sum_{i=1}^{N} T_i \tag{1}$$

$$T_i = \tfrac{1}{2}\int \rho_i V_i^T V_i dy. \tag{2}$$

The velocity of a point on the panel is given by $V_i = \dot{r}_i + \omega \times r_i$ where $r_i^T = [0 \;\; a_i + y_i - \vartheta_i \;\; w_i]$, where ϑ_i is the displacement of the ith in the ϑ direction. Replacing appendage velocity in the kinetic energy results in

$$T_i = \tfrac{1}{2}\int (\omega^T I_i \omega + \kappa_i \omega + \rho_i \dot{w}_i^2) dy \tag{3}$$

where I_i is the inertia tensor of the ith appendage, I_c is the inertia tensor of the rigid hub, κ_i is the ith appendage angular momentum due to the flexibility, and w_i is the deflection in the $-z$ direction of the appendage reference frame.

The attitude dynamic equation is given by

$$\frac{dH}{dt} + \omega \times H = \tau, \qquad H = \frac{\partial T}{\partial \omega} + h_\omega \tag{4}$$

where τ is the control torque and h_ω is the internal angular momentum due to rotating wheels. The final form of the flexible attitude dynamic equation is then given by

$$I_t \dot{\omega} + \dot{I}_t \omega + \Omega(I_t \omega + \kappa_t + h_\omega) + \dot{\kappa}_t = \tau \tag{5}$$

where Ω is a skew symmetric matrix associated with the angular velocity vector ω and $\kappa_t = \sum_{i=1}^{N} \kappa_i$. To simplify the analysis, $\dot{\kappa}_t$ is divided to two terms, namely: $\dot{\kappa}_t = \dot{\kappa}_{\ddot{q}} \ddot{q} + \dot{\kappa}_{\dot{q}}$.

To derive the dynamic model of the described system, the assumed modes formulation of the flexible appendage dynamics is used. Flexible deflection of the appendages along the body axis is given by

$$w_i = w_i(y,t) = \sum_{j=1}^{n} q_j(t)\psi_j(y_i) = \psi_i q_i \tag{6}$$

where q_i are modal coordinates, n is the number of assumed modes, and ψ_i are the shape functions of the appendage deformation.

The mode shape functions for the clamped-free beams $\psi_s(y)$ is given by

$$\psi_s(y) = \left\{ \left[\cosh\left(\lambda_s \frac{y}{l}\right) - \cos\left(\lambda_s \frac{y}{l}\right) \right] - \sigma_s \left[\sinh\left(\lambda_s \frac{y}{l}\right) - \sin\left(\lambda_s \frac{y}{l}\right) \right] \right\} \tag{7}$$

$$\sigma_s = \frac{\sinh(\lambda_s) - \sin(\lambda_s)}{\cosh(\lambda_s) + \cos(\lambda_s)} \tag{8}$$

where λ_s is a root of $\cosh(\lambda_s) + \cos(\lambda_s) + 1 = 0$.

The potential energy does not include a gravity term and is just the usual potential energy of beam bending deformation:

$$P = \sum_{i=1}^{N} \int E_i I_i y_i''^2 dy = \sum_{i=1}^{N} \frac{E_i h_i^3}{12(1-\gamma_i^2)} \int q_i \psi_i''^T \psi_i'' q_i dy \tag{9}$$

where h_i, γ_i and E_i are the thickness, the Poisson ratio, and the modulus of the elasticity of the ith appendage, respectively.

The vibration equations of motion are obtained by using the conventional form of Lagrange's equation:

$$\frac{d}{dt}\left(\frac{\partial T}{\partial \dot{q}_{is}}\right) - \frac{\partial T}{\partial q_{is}} + \frac{\partial P}{\partial q_{is}} = 0. \tag{10}$$

Substituting the kinetic and potential energy equations in the Lagrange's equation, the final form of the vibration equation for the ith appendages is obtained:

$$M_{\psi\psi}\ddot{q} + \dot{\kappa}_q^T \dot{\omega} = Kq + D\dot{q} + C. \tag{11}$$

The vectors and matrices in the expressions above are obtained from integrals of the appendages mode shapes and their spatial derivatives which are given in the Appendix.

The final form of equation is given by augmenting (5) and (11) and using $\dot{\kappa}_t = \dot{\kappa}_{\ddot{q}}\ddot{q} + \dot{\kappa}_{\dot{q}}$:

$$\begin{bmatrix} I_t & \dot{\kappa}_{\ddot{q}} \\ \dot{\kappa}_{\ddot{q}}^T & M_{\psi\psi} \end{bmatrix} \begin{bmatrix} \dot{\omega} \\ \ddot{q} \end{bmatrix} = \begin{bmatrix} -(\dot{I}_t \omega + \Omega(I_t \omega + \kappa_t h_\omega) + \dot{\kappa}_{\dot{q}}) \\ Kq + D\dot{q} + C \end{bmatrix} + \begin{bmatrix} \tau \\ 0 \end{bmatrix}. \tag{12}$$

To include structural damping, a viscous damping term is added to (11) which results in a diagonal damping matrix D, with entries ζ for the damping parameter.

III. OUTPUT REDEFINITION APPROACH

It is well known that the zero dynamics of a flexible spacecraft associated with the panel deflection are unstable. In other words, the system is nonminimum phase and is very difficult to control using panel deflection output for feedback.

The goal is to control attitude angles and panel deflection of flexible spacecraft. The Euler parameter θ is used for attitude representation of body fixed frame with respect to an inertia frame; we have

$$\dot{\theta} = R\omega \tag{13}$$

$$R^{-1} = \begin{bmatrix} 1 & 0 & -\sin\theta_2 \\ 0 & \cos\theta_1 & \sin\theta_1 \cos\theta_2 \\ 0 & -\sin\theta_1 & \cos\theta_1 \cos\theta_2 \end{bmatrix}. \tag{14}$$

In [10] the sum of the joint angle and a scaling of the tip elastic deformation is chosen as the output for control of a flexible link manipulator, namely, $y_{ai} = \theta_i + \alpha_i q_i$, where $-1 \le \alpha_i \le 1$. For the choice of $\alpha_i = 1$, the output becomes the tip angular position and for $\alpha_i = 0$ the output becomes the joint angle.

Moreover, it was shown that a critical value α_i^*, $0 \prec \alpha_i^* \prec 1$ exists such that the zero dynamics

related to the new output y_a are unstable for all $\alpha_i^* \prec \alpha_i$ and are stable for $-1 \le \alpha_i \le \alpha_i^*$. Our objective in this section is to show that by using the new output y_{ai}, the dynamics of the flexible spacecraft may be expressed in such a way that the feedback linearization method is applicable for controlling the system.

The dynamic equation for flexible spacecraft with one panel and considering one elastic mode is of 8th order. Let us define the output as $y = \theta + \alpha q$. Now by differentiating y twice along the trajectory of the system, an explicit relationship between the output y and controller input τ would be obtained. Hence it is apparent that the system relative degree is $r = 6 < n = 8$.

Therefore, parts of the system dynamics have been rendered "unobservable" in this input-output linearization, the so-called internal dynamics of the system, since it cannot be seen from the external input-output relationship.

Consider the dynamics of the spacecraft (12) expressed in standard state space form $\dot{x} = f(x) + g(x)\tau$. The new set of states can be defined by $X = [\theta \;\; q \;\; \dot{\theta} \;\; \dot{q}]$. Choosing the state vector as x, the corresponding vector fields f and g can be written as

$$f(x) = \begin{bmatrix} R\omega \\ \dot{R}\omega + RA_\omega(-I_\omega - \dot{\kappa}_{\ddot{q}} M_{\psi\psi}^{-1}(Kq + C)) \\ \dot{q} \\ M_{\psi\psi}^{-1}((\dot{\kappa}_{\ddot{q}} A_\omega \dot{\kappa}_{\ddot{q}} M_{\psi\psi}^{-1} + 1)(Kq + C) + \dot{\kappa}_{\ddot{q}} A_\omega I_\omega) \end{bmatrix} \tag{15}$$

$$g(x) = [0 \quad R \quad A_\omega \quad 0 \quad -M_{\psi\psi}^{-1}\dot{\kappa}_{\ddot{q}} A_\omega] \tag{16}$$

$$A_\omega = (I_t - \dot{\kappa}_{\ddot{q}} M_{\psi\psi}^{-1}\dot{\kappa}_{\ddot{q}})^{-1}, \qquad I_\omega = (\dot{I}_t\omega + \Omega(I_t\omega + \kappa_t h_\omega) + \dot{\kappa}_{\dot{q}}). \tag{17}$$

The new output can be expressed as $y = \theta + \alpha q$. To find the external dynamics related to this new output, take $\mu_1 = \theta + \alpha q$ and $\mu_2 = \dot{\theta} + \alpha\dot{q}$. From (15) and (16), we can write

$$\dot{\mu}_1 = \mu_2 \tag{18}$$

$$\dot{\mu}_2 = \ddot{\theta} + \alpha\ddot{q} = (f_2 + \alpha f_4) + (g_2 + \alpha g_4)\tau. \tag{19}$$

The function $\psi(x)$ is required to complete the transformation, i.e., it brings the dynamics to its normal form. The third function $\psi(x)$ should satisfy the following equation [15]:

$$L_{g_j}\psi_k = \left(\frac{\partial \psi_k}{\partial x}\right) g_j = 0 \tag{20}$$

$$\left(\frac{\partial \psi_i}{\partial \dot{\theta}}\right) RA_\omega + \left(\frac{\partial \psi_i}{\partial \dot{q}}\right)(M_{\psi\psi}^{-1}\dot{\kappa}_{\ddot{q}} A_\omega) = 0. \tag{21}$$

One solution for this equation is

$$\psi_1 = q, \qquad \psi_2 = M_{\psi\psi}^{-1}\dot{\kappa}_{\ddot{q}} R^{-1}\dot{\theta} + \dot{q}. \tag{22}$$

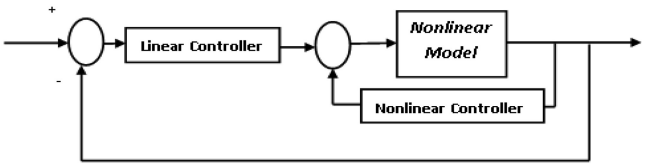

Fig. 2. Feedback linearization method.

By differentiating these functions and by using system dynamics (15), the internal dynamics can be obtained as

$$\dot{\psi}_1 = \dot{q}, \qquad \dot{\psi}_2 = M_{\psi\psi}^{-1}(K(\mu_2) + C(\mu_2) + D(\zeta)\psi_1) \tag{23}$$

It is shown that local asymptotic stability of zero dynamics is enough to guarantee the local asymptotic stability of the internal dynamics [15]. The zero dynamics is defined to be the internal dynamics of the system when the system output is kept identically at zero by a proper input.

$$\dot{\psi}(0, \psi) = w(0, \psi) \tag{24}$$

$$y = 0 \rightarrow \dot{\theta} = -\alpha\dot{q}. \tag{25}$$

Using the system dynamics (12), we have

$$\ddot{q} = -M_{\psi\psi}^{-1}\dot{\kappa}_{\ddot{q}}\dot{\omega} + M_{\psi\psi}^{-1}(Kq + D\dot{q} + C). \tag{26}$$

Using (22) and (13), (25)–(26), it follows that

$$(I - M_{\psi\psi}^{-1}\dot{\kappa}_{\ddot{q}} R^{-1}\alpha)\ddot{\psi}_1 + (M_{\psi\psi}^{-1}\dot{\kappa}_{\ddot{q}} R^{-1}\dot{R}R^{-1}\alpha + M_{\psi\psi}^{-1} D)\dot{\psi}_1 + M_{\psi\psi}^{-1} K\psi_1 + M_{\psi\psi}^{-1} C = 0 \tag{27}$$

where I is an $N \times N$ identity matrix. Since $(I - M_{\psi\psi}^{-1} \cdot \dot{\kappa}_{\ddot{q}} R^{-1}\alpha)$ could be made positive by a proper selection of α, we can conclude that the zero dynamics can be made asymptotically stable. Note that α is a $3 \times N$ matrix. However the structures of $M_{\psi\psi}$ and $\dot{\kappa}_{\ddot{q}}$ given in the Appendix reveal that $M_{\psi\psi}$ is a diagonal matrix and $\dot{\kappa}_{\ddot{q}}$ is a vector with only one component in each row being non-zero. Hence, only one component in each row of α has to be selected. Given the numerical parameters, α could be readily obtained.

IV. THE FEDDBACK LINEARIZATION CONTROLLER

It is assumed that no actuator is available on the flexible beam-type appendages. It is well known that in such cases flexible beam is not input-state linearizable and we must turn to the input-output feedback linearization (or the so-called dynamic inversion) control technique, (see Fig. 2). It is assumed that full state measurement of the system is available through attitude (e.g. sun sensors, gyros, and accelerometers).

The successive differentiation process is done on the output (attitude angle) until the control signal

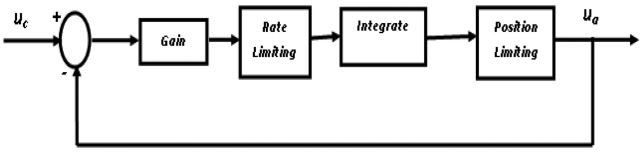

Fig. 3. Enforcing control saturation limits.

appears

$$y = \theta + \alpha q \xrightarrow{\text{yields}} \ddot{y} = \ddot{\theta} + \alpha \ddot{q} = \nu. \tag{28}$$

Using dynamic equations of spacecraft (12), it follows that

$$\ddot{y} = \ddot{\theta} + \alpha \ddot{q} = (f_2 + \alpha f_4) + (g_2 + \alpha g_4)\tau. \tag{29}$$

The coefficient of τ, A_ω, in the special case ($q = 0$) is equal to I_c^{-1}; in other cases, it can be shown that this term is also invertible. Hence the signal ν should be constructed to control the linearized system. The system can be controlled by introducing linear controller of the form:

$$\upsilon = \omega_y^2 y_e - 2\varsigma_y \omega_\theta \dot{y}_e. \tag{30}$$

In most modern spacecraft, momentum exchange devices are used as actuators. Due to saturation effect in these actuators, considering saturation is very important. It has been shown by several authors that enforcing actuator constraints for input-output linearization can result in poor closed-loop performance (when compared with unconstrained closed-loop performance) [16–17]. Different methods have been successfully demonstrated that assist in preventing the destabilizing effects of control saturations in feedback linearization method. In most cases, saturation is considered by designing a special outer loop (linear) controller; hence these methods cannot be used in this paper because of defined outer loop, μ-synthesis method. To enforce the position and rate saturation limits, feedback controller structures are used in [18]–[19]. Most of these structures filter the peak of the response. Simulation studies show considering the saturation in inner and outer loop together is more effective. In this paper the structure shown in Fig. 3 is used [18]. The gain can be chosen depending on the bounds of output response. In appropriate scaling, tanh can be used to represent saturation behavior:

$$\tau_{\text{sat}} = \tanh(\tau/\tau_{\max})\tau_{\max} \tag{31}$$

where τ_{sat} is the saturation limit of the actuator. Let us define the following parameters:

$$A_1 = f_2 + \alpha f_4 \tag{32}$$

$$A_2 = g_2 + \alpha g_4. \tag{33}$$

Equation (19) can be written as

$$\ddot{y} = A_1 + A_2\tau. \tag{34}$$

Let δ be the difference between the computed control τ_c and the applied control τ_a:

$$\delta = \tau_c - \tau_a. \tag{35}$$

From (34) and (35), we have

$$\ddot{y} = A_1 + A_2(\tau + \delta). \tag{36}$$

Then, the linearized model takes the following form:

$$\ddot{y} = \upsilon + A_2\delta. \tag{37}$$

As shown in (37), the hedge signal $A_1\delta$ acts as a disturbance to the system equations.

V. THE PROPOSED COMPOSITE CONTROLLER (FEEDBACK LINEARIZATION + μ-SYNTHESIS)

The performance of feedback linearization is rather poor in the presence of uncertainty, disturbance, and noise. Due to the uncertainty, inexact dynamic cancelation arises in the inner-loop feedback linearization design. Hence a μ-synthesis control law is added as an outer-loop linear controller. Dynamic inversion and structured singular value synthesis are combined to achieve robust control of flexible spacecraft. The controller structure is shown in Fig. 2. In this method nonlinear dynamics are linearized by input-output feedback linearization method. By definition output as $y = \theta + \alpha q$, the new linear system is in the form of $\ddot{y} = \nu$; so a new control signal ν should be designed.

The advantage of μ-synthesis method is that it allows the direct inclusion of modeling errors or uncertainties, measurement and control inaccuracies, and performance requirements into a common control problem formulation.

By the definition of two parameters A_1 and A_2 as expressed in relations (32)–(33), we have

$$\ddot{y} = A_2\tau + A_1 = \upsilon_{\text{real}}. \tag{38}$$

By considering uncertainty on parameters such as I_c, (38) can be written as

$$\begin{aligned}\ddot{y} &= (A_2 + \Delta A_2)\tau + (A_1 + \Delta A_1) \\ &= A_2\tau + A_1 + \Delta A_2\tau + \Delta A_1 = \upsilon_{\text{real}} + \Delta\upsilon \end{aligned} \tag{39}$$

$$\Delta\upsilon = \Delta A_2\tau + \Delta A_1 = \Delta A_2 A_2^{-1}(\upsilon_{\text{real}} - A_1) + \Delta A_1. \tag{40}$$

By substituting real parameters, (39) can be written as

$$\begin{aligned}\ddot{y} &= \upsilon_{\text{real}} + \Delta A_2 A_2^{-1}(\upsilon_{\text{real}} - A_1) + \Delta A_1 \\ &= \upsilon_{\text{real}} + \Delta A_2 A_2^{-1}\upsilon_{\text{real}} - \Delta A_2 A_2^{-1} A_1 + \Delta A_1. \end{aligned} \tag{41}$$

As (41) shows, parameter uncertainty results in a multiplicative uncertainty in controller input ($\Delta A_2 A_2^{-1}$) and a disturbance ($-\Delta A_2 A_2^{-1} A_1 + \Delta A_1$). The controller structure is shown in Fig. 4.

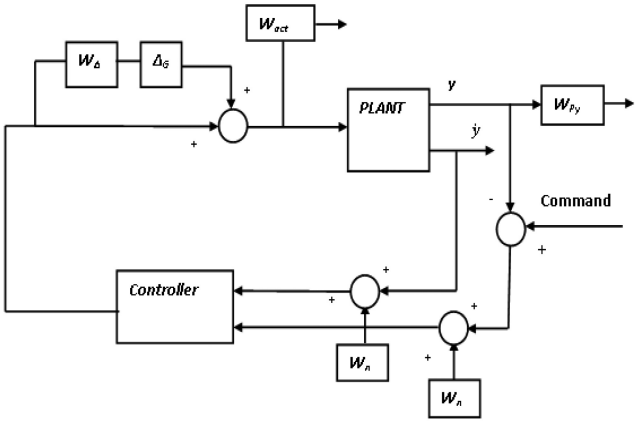

Fig. 4. μ-synthesis arrangement block diagram.

To include the uncertainty in the model, different system parameters such as I_c were perturbed by 20% of their nominal values. Then, the nominal transfer function $(1/s^2)$ of the system was selected as a double integrator, i.e., $1/s^2$. Then the bode diagram of the actual system and the nominal transfer function plus the multiplicative weighting functions were obtained. The weighting functions were then tuned to get the best possible match which is obtained for $W_\Delta = 70(s+1)/(s+100)$.

The effect of uncertain parameters on transfer function and bounds of selected weight is shown in Fig. 5. W_p weights the error between complementary sensitivity function of the closed-loop system and an ideal model of system response. The performance objective can be written as $|W_P S| < 1$, so W_p should be selected such as $W_P \prec 1/|S|$. According to the first and third frequency of the vibration modes of the flexible panel, this function is chosen as: $W_{p\theta} = 0.1(s^2+s+0.25)/(s^2+4s+0.01)$. Therefore the hub performance weight has a relatively large magnitude at low frequencies.

According to the weakness of the dynamic inversion method against constant disturbance, a disturbance weight is chosen such as: $W_{\text{dist}}/|\upsilon| = W_{\text{distact}}/|\tau|$.

W_{distact} of constant magnitude equal to 0.001 is applied to the system. The parametric uncertainty disturbance in (41) is very small, so in comparison it isn't considered.

To enforce the controller saturation limits in the inner loop, the feedback controller structure shown in Fig. 3 is used. Also, this saturation can be considered in designing the μ-synthesis controller; however using the dynamic inversion formulation, the actuator dynamics is not directly accessible. In [13] an algorithm is derived to catch bound on ν in the feedback linearization outer loop according to actuator saturation limit. In this paper this limit is approximately obtained according to the following equation by assuming small q:

$$\begin{aligned}\upsilon &= (f_2+\alpha f_4)+(g_2+\alpha g_4)\tau \\ &= \dot{R}\omega + RA_\omega(\tau - I_\omega - \dot{\kappa}_{\ddot{q}} M_{\psi\psi}^{-1}(Kq+C)) + \alpha M_{\psi\psi}^{-1} \\ &\quad \times ((\dot{\kappa}_{\ddot{q}} A_\omega \dot{\kappa}_{\ddot{q}} M_{\psi\psi}^{-1} + 1)(Kq+C) - \dot{\kappa}_{\ddot{q}} A_\omega I_\omega) \\ &\quad - \alpha A_\omega \dot{\kappa}_{\ddot{q}} M_{\psi\psi}^{-1}. \end{aligned} \tag{42}$$

According to actuator saturation limitation $|\tau| <$ 0.8 N.m, it is chosen as $W_{\text{act}} = 4000$.

The weighting noise function W_n is used to model sensor noise since all of the feedback signals are corrupted to some extent by noise. It is assumed that the angular velocity and the pitch angle are measured by rate gyro and Earth sensor that are corrupted with random measurement noise of magnitude 0.1 deg/s and 0.2 deg. W_n is a high-pass filter according to high frequency noise nature.

$$W_n = \left(\frac{0.2\pi}{180}\right)\frac{0.12s+1}{0.001s+1}.$$

A concern is that as the number of states in the problem formulation increases, the accuracy of the numerical solution decreases. So in this paper the controller is designed using attitude and rate of attitude feedback.

With regard to many signal inputs of controller and performance requirements (robustness against noise, disturbance, uncertainty, and actuator saturation in this complex system), the resulting controller is of high order. This is obviously not practical for application; it can be reduced tremendously without

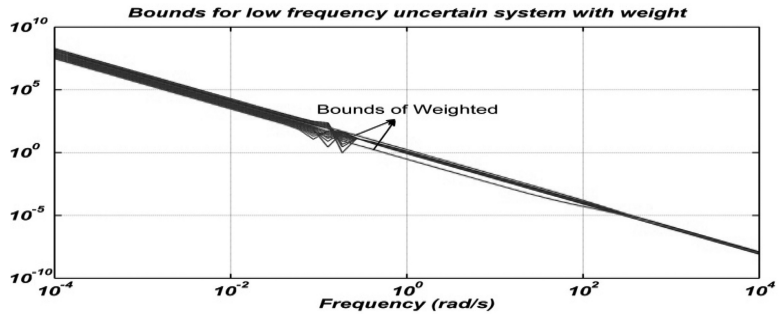

Fig. 5. Bounded of uncertainties and chosen weight.

degrading much of the performance. Using balanced truncation, the order is reduced without much loss of closed-loop performance or robustness.

α is chosen such that system zero dynamic be stable. Hence, the internal dynamic is stable. Considering μ of outer loop less than 1, the system is stable.

VI. SIMULATION RESULTS

In this section, simulation results for the closed-loop system (12) with the control laws derived in the previous sections are presented using MATLAB and SIMULINK software. In the simulation, the system parameters are chosen the same as those in [1].

$$E = 5 * 10^8 \text{ N/m}^2, \qquad \rho = 8 \text{ kg/m}$$
$$l = 10 \text{ m}, \qquad r = [0 \;\; 0.5 \;\; 0] \text{ m} \tag{43}$$
$$h = 0.02 \text{ m}, \qquad I_c = \begin{bmatrix} 400 & 3 & 10 \\ 3 & 300 & 12 \\ 10 & 12 & 200 \end{bmatrix} \text{ kg/m}^2.$$

The control input and its rate is bounded as

$$|u| \prec 0.8 \text{ N.m}, \qquad |\dot{u}| \prec 0.8 \text{ N.m/s}. \tag{44}$$

The environmental disturbances (i.e., gravity gradient, solar pressure, aerodynamic and magnetic torques) on the spacecraft are obtained from the following equation:

$$\tau_d = \begin{bmatrix} 0.005 - 0.05 \sin\left(\dfrac{2\pi t}{400}\right) + \delta(200, 0.2) + \nu_1 \\ 0.005 + 0.05 \sin\left(\dfrac{2\pi t}{400}\right) + \delta(250, 0.2) + \nu_2 \\ 0.005 - 0.03 \sin\left(\dfrac{2\pi t}{400}\right) + \delta(300, 0.2) + \nu_3 \end{bmatrix} \quad \text{[N.m]} \tag{45}$$

where $\delta(T, \Delta T)$ denotes an impulsive disturbance with magnitude 1, period T, and width ΔT. The terms ν_1, ν_2, and ν_3 denote white Gaussian noises with mean values of 0 and variances of 0.005^2.

It is assumed that the angular velocity and the pitch angle are measured by rate gyro and Earth sensor, respectively, that are corrupted with random measurement noise. Earth sensor noise has Gaussian distribution, zero mean, and standard deviation of 0.2 deg. The gyro noise sources correspond to a random drift rate and a random bias rate. This model is represented by the following Laplace transformed equation:

$$\omega_M = H_{\text{gyro}}\omega + \omega_D + \omega_N \tag{46}$$

where ω_M and ω are the measured and actual spacecraft angular velocity, respectively. Gyro random bias rate ω_N and Gyro random drift noise ω_D have Gaussian distribution, with zero mean, and standard deviation of 10^{-6} rad/s. Gyro transfer function is

$$H_{\text{gyro}} = (4469s + 89.22)/(s^3 + 89.22s^2 + 4469s + 89.22). \tag{47}$$

Velocity and acceleration of a point on the flexible panel is measured by a tachometer and accelerometers with Gaussian distribution noise, zero mean, and standard deviation of 0.0001 m/s and 0.0001 m/s^2, respectively. The robustness specification is to account for variation on the values of I_c and $M_{\psi\psi}$ in (12) which would represents the model parameter uncertainties in the system up to 20%.

In this paper the coefficient $\dot{\kappa}_{\ddot{q}} M_{\psi\psi}^{-1}$, by considering one elastic mode, is equal to [6.0804 0 0]; α should be chosen less than its inverse. In simulations this constant is chosen as: α = [0.14 0.14 0.14]. By considering a more elastic mode, i.e., three, this coefficient is

$$\begin{bmatrix} 6.0804 & 0 & 0 \\ 1.1247 & 0 & 0 \\ 0.4514 & 0 & 0 \end{bmatrix}$$

hence for higher elastic mode, we can chose larger α.

The first three natural frequencies in our simulations are $\omega_1 = 11.89$, $\omega_2 = 74.55$, and $\omega_3 = 208.75$ (rad/s).

Also, the gain parameters in the feedback linearization method are chosen as $\omega_y = 0.015$, $\xi_y = 1$. In this subsection, a comparison of robustness obtained for the nonlinear system with the two proposed controllers (1—feedback linearization, 2—combination of feedback linearization and μ-synthesis) are presented.

A number of time and frequency domain analysis procedures are carried out on the resulting designs and their performances are tested. In all simulations no damping is considered.

The results for the classical feedback linearization and composite controller are given in Figs. 6–7, respectively.

A. Feedback Linearization Controller

Fig. 6 shows the simulation results of the feedback linearization controller. As compared with Figs. 6(a) and 7(a), in normal conditions or in conditions where only one finite uncertain variation (disturbance, noise and uncertainty) exists, this method responds very well. It means the feedback lineariztion design leads to smaller maximum overshoot and complete suppression of panel deflection. The dynamic inversion controller achieves this decoupling at the cost of larger and faster control effort (comparing Figs. 6(c) and 7(c)).

However in a large maneuver or in combined uncertain conditions (several uncertain conditions

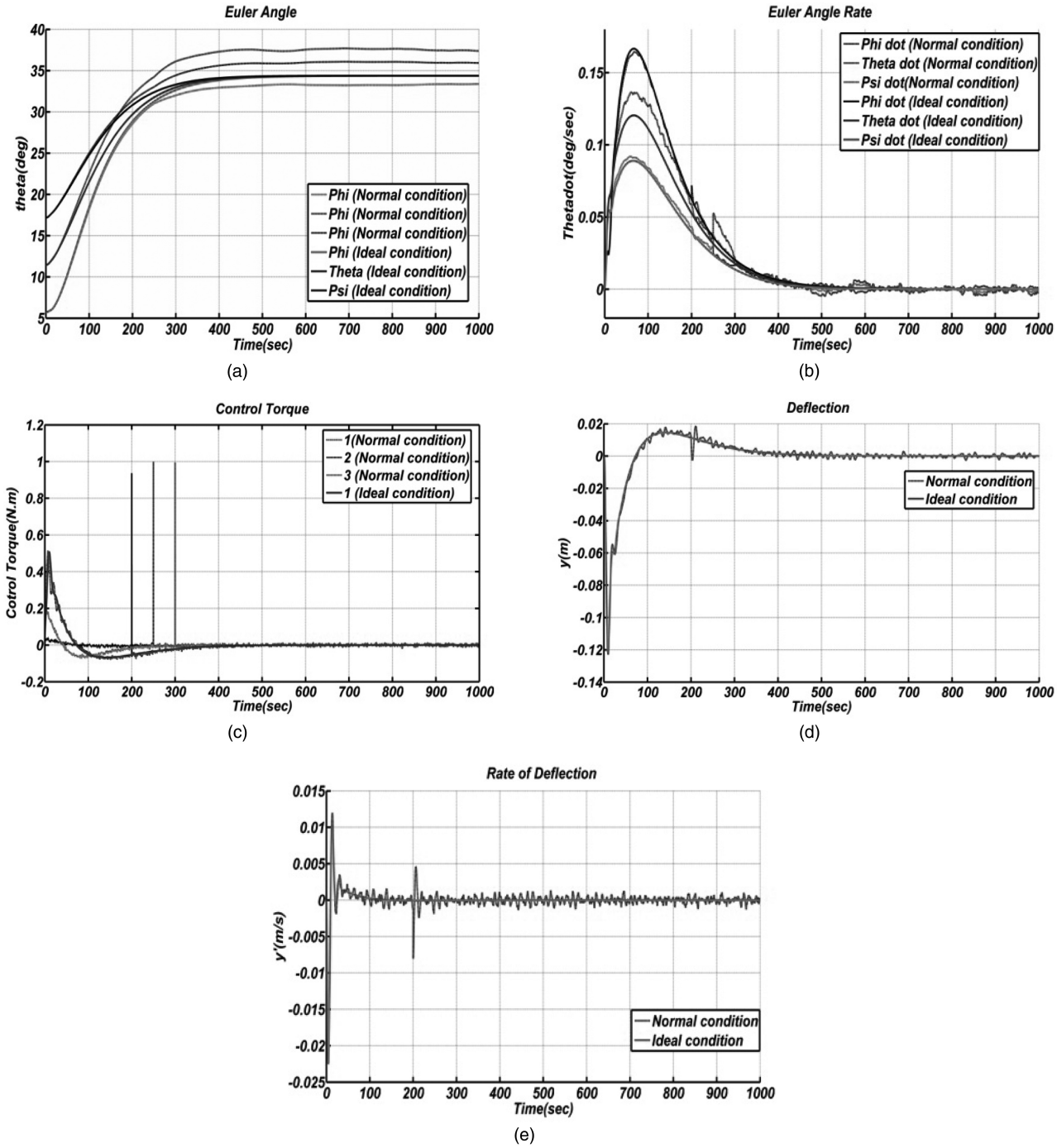

Fig. 6. Dynamic inversion method. (a) Spacecraft attitude (Euler angles). (b) Angular velocity. (c) Reaction wheel torque. (d) Tip deflection. (e) Tip rate.

exist together or one uncertain condition with larger variations), as shown in Fig. 6, much larger control efforts are necessary (out of maximum acceptable control input) and the attitude rate and position cannot converge.

B. Composite Controller

Fig. 7 shows the simulation results of the composite controller. With the designed composite algorithm, the response of roll, pitch, and yaw angles are shown in Fig. 7(a). We can see that each of the three attitude angles approaches reference trajectory at time of 600 s. Hence fast and precise attitude control is achieved for the current design system. As compared with Fig. 6(a) (uncertain condition), in the dynamic inversion method the response has a large steady state error and cannot converge.

Fig. 7(d) shows low frequency oscillation of the appendage in the composite method. The maximum

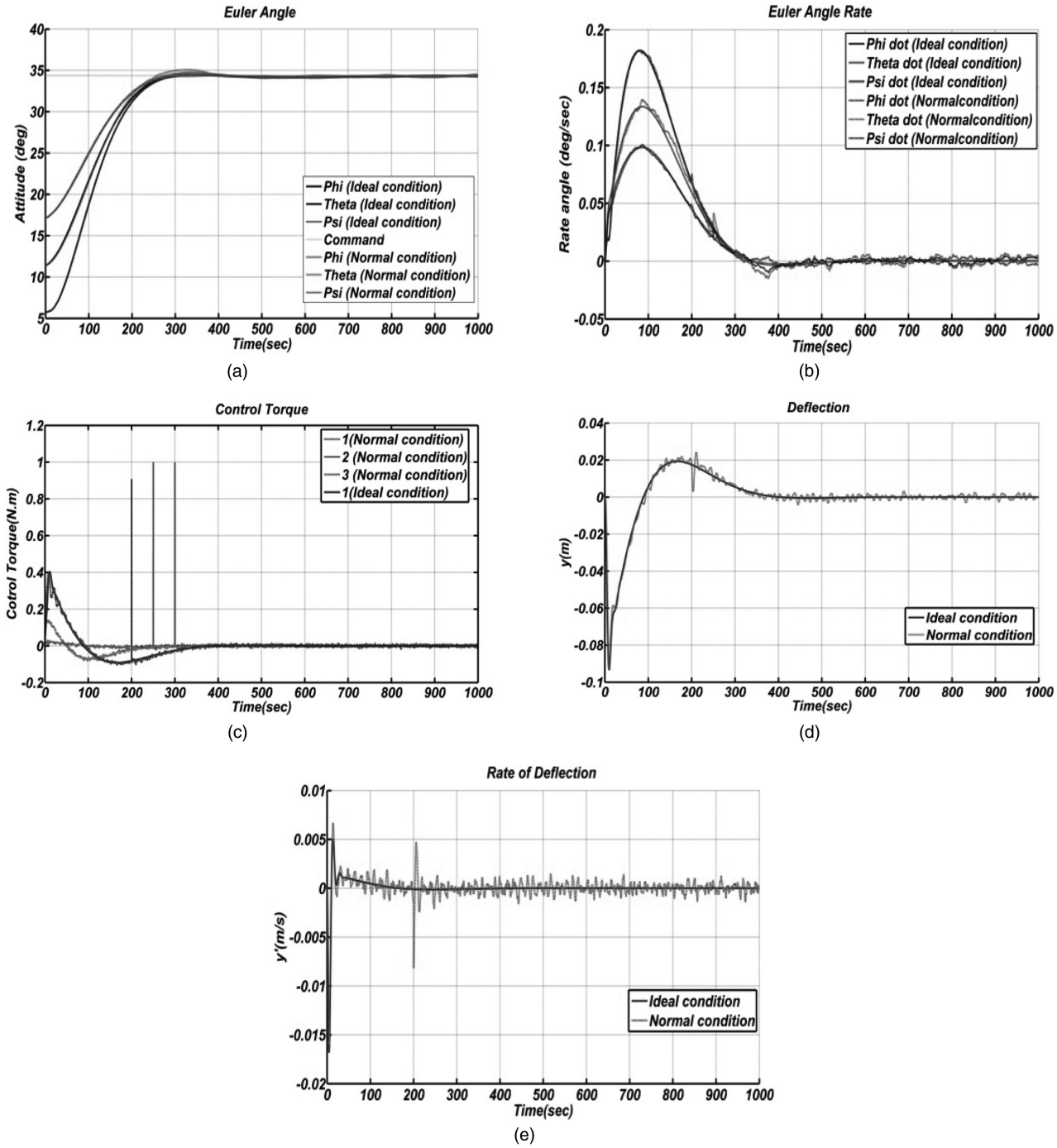

Fig. 7. Composite method. (a) Spacecraft attitude (Euler angles). (b) Angular velocity. (c) Reaction wheel torque. (d) Tip deflection. (e) Tip rate.

tip deflection of the appendage is larger in the dynamic inversion method and can be seen to be around 0.16 m (Fig. 6(d), with uncertainty). Overall, comparing the plots 7(e) and 6(e), the composite controller has a larger rate of tip deflection caused by faster panel deflection damping.

Requirement for momentum of each reaction wheel is illustrated in Fig. 7(c). As compared with Fig. 6(c), the composite method requires larger controller effort. Simulations show the composite control algorithm performs well in large maneuvers; however it has a larger controller order.

The simulation results by the composite controller when $\alpha = 0$ (means the system output is only hub angles) show the ability of the output redefinition method used.

VII. CONCLUSIONS

Vibration attenuation is a challenging control problem due to the stringent requirements on the

performance and inherent characteristics of such structures. In this paper flexible spacecraft attitude has been controlled by two controller designs. The first controller is the dynamic inversion; the second is a combination of dynamic inversion and μ-synthesis controller. The controllers have been designed by utilizing the modified output redefinition approach. It is assumed that only three torques in three directions on the hub are used. Actuator saturation is considered in the design of the controllers. At first the performance of the two designs were compared in areas such as speed of response, damping of panel vibration modes, and size of control deflection used. In the next step the robustness of the two designs to uncertainty was examined. Finally, the sensitivity of the controllers to measurement noise, environment disturbance, and large maneuvers was compared.

Simulation results prove the composite controller ability in controlling attitude and suppressing the vibration of panels with excellent performance and robustness for a broad range of operating conditions with minimal control effort.

It is important to note that these controllers damp vibration of panels without considering a damping term and without using any filter. In this paper it is assumed that sensor noise, disturbance, and uncertainty to be close to real values. It is notable that this composite control method has never been used on spacecraft and that all terms such as disturbance, noise, uncertainty, nonlinearity and saturation, are rarely simultaneously considered in the simulations of flexible spacecraft.

APPENDIX

The vectors and matrices in (21) can be written as follows

$$I_t = I_c + \sum_{i=1}^{N} I_i, \qquad \kappa_t = \sum_{i=1}^{N} \kappa_i \tag{48}$$

$$C = \rho_i[-\omega_y\omega_z(a_i m_\psi + m_{\psi y})] \tag{49}$$

$$K = \rho_i \left((M_{\psi\psi} - a_i M_{\psi'\psi'\eta} - M_{y\psi'\psi'\eta})\omega_x^2 - (a_i M_{\psi'\psi'\eta} - M_{y\psi'\psi'\eta})\omega_z^2 - \frac{2EI}{\rho_i} M_{\psi''\psi''} \right). \tag{50}$$

The displacement in the ϑ direction can be found to be

$$\vartheta = \frac{1}{2}\int_0^y \left(\frac{\partial w_i(\eta,t)}{\partial \eta}\right)^2 d\eta = \frac{1}{2}\int_0^y q^T \psi'(\eta)\psi'(\eta) q\, d\eta. \tag{51}$$

Substituting w and ϑ in the formulation of I and κ and neglecting the high order term, the final values in the ith panel are obtained as

$$I_{xx} = \rho l\left(a^2 + \frac{l^2}{3} + al\right) + \rho(q^T M_{\psi\psi} q - aq^T M_{\psi'\psi'\eta} q - q^T M_{y\psi'\psi'\eta} q \tag{52}$$

$$I_{xy} = 0, \qquad I_{xz} = 0 \tag{53}$$

$$I_{yy} = \rho(q^T M_{\psi\psi} q) \tag{54}$$

$$I_{yz} = \rho(-am_\psi q - m_{\psi y} q) \tag{55}$$

$$I_{zz} = \rho l\left(a^2 + \frac{l^2}{3} + l\right) - \rho(aq^T M_{\psi'\psi'\eta} q + q^T M_{y\psi'\psi'\eta} q) \tag{56}$$

$$\kappa = \begin{bmatrix} \rho(am_\psi \dot{q} - m_{\psi y}\dot{q}) \\ 0 \\ 0 \end{bmatrix}. \tag{57}$$

Mode shape integrals resulting from Lagrangian were derived analytically and are provided here:

$$M_{\psi''\psi''} = \begin{cases} \dfrac{\lambda_i^4}{l^3}, & i = j \\ 0, & i \neq j \end{cases}, \qquad M_{\psi\psi} = \begin{cases} l, & i = j \\ 0, & i \neq j \end{cases} \tag{58}$$

$$M_{\psi'\psi'\eta} = \begin{cases} 2 + \dfrac{\sigma_i^2\lambda_i^2}{2} - \sigma_i\lambda_i, & i = j \\ \dfrac{8\lambda_i^2\lambda_j^2}{(\lambda_j^2 + (-1)^{i+j}\lambda_i^2)^2} - \dfrac{4\lambda_i^2\lambda_j^2(\sigma_j\lambda_j - \sigma_i\lambda_i)}{(\lambda_j^4 - \lambda_i^4)}, & i \neq j \end{cases} \tag{59}$$

$$m_\psi = \frac{2l\sigma_i}{\lambda_i}, \qquad m_{\psi y} = \frac{2l^2}{\lambda_i^2}. \tag{60}$$

Further details can be found in [1].

REFERENCES

[1] Tafazoli, S. and Khorasani, K.
Nonlinear control and stability analysis of spacecraft attitude recovery.
IEEE Transactions on Aerospace and Electronic Systems, **42**, 3 (2006), 825–845.

[2] Karkoub, M. A., et al.
Robust control of flexible manipulators via μ-synthesis.
Control Engineering Practice, **8** (2000), 725–734.

[3] Zheng, J., Banks, S. P., and Alleyne, H.
Optimal attitude control for three-axis stabilized flexible spacecraft.
Acta Astronautica, **56** (2005), 519–528.

[4] Uang, H. J. and Lien, C. C.
Mixed H2/H8 PID tracking control design for uncertain spacecraft systems using a cerebella model articulation controller.
IEE Proceedings—Control Theory Application, **153** (Jan. 2006), 1–13.

[5] Chen, B. C., Wu, C. S., and Jan, Y. W.
Adaptive fuzzy mixed H2/H8 attitude control of spacecraft.
IEEE Transactions on Aerospace and Electronic Systems, **36**, 4 (Oct. 2000), 1343–1359.

[6] Wu, C. S. and Chen, B. S.
Adaptive attitude control of spacecraft mixed H2/H8 approach.
Journal of Guidance, Control and Dynamics, **24**, 4 (July–Aug. 2001), 755–766.

[7] Show, L. L., Juang, J. C., and Jan, Y. W.
An LMI-based nonlinear attitude control approach.
IEEE Transactions on Control Systems Technology, **11**, 1 (Jan. 2003), 73–83.

[8] Kim, L. S. and Kim, Y.
Robust backstepping control for slew maneuver using nonlinear tracking function.
IEEE Transactions on Control Systems Technology, **11**, 6 (Nov. 2003), 822–829.

[9] Zhang, R. and Singh, S. N.
Adaptive output feedback control of spacecraft with flexible appendages.
In *IEEE Proceedings of The American Control Conference*, Arlington, VA, June 25–27, 2001.

[10] Luo, W., Chu, Y. C., and Ling, K. V.
Inverse optimal adaptive control for attitude tracking of spacecraft.
IEEE Transactions on Automatic Control, **50**, 11 (Nov. 2005), 1639–1654.

[11] Li, Z. B., Wang, Z. L., and Li, J. F.
A hybrid control scheme of adaptive and variable structure for flexible spacecraft.
Aerospace Science and Technology, **8** (2004), 423–430.

[12] Singh, S. N. and Yim, W.
Nonlinear adaptive spacecraft attitude control using solar radiation pressure.
IEEE Transactions on Aerospace and Electronic Systems, **41**, 3 (July 2005), 70–779.

[13] Mahdavan, S. K. and Singh, S. N.
Inverse trajectory control and zero dynamic sensitivity of an elastic manipulator.
International Journal of Robotics and Automation, **6**, 4 (1991), 179–191.

[14] Talebi, H. A., Khorasani, K., and Patel, R. V.
Neural network based control schemes for flexible-link manipulators: Simulations and experiments.
Neural Networks, **11** (1991), 1357–1377.

[15] Slotine, J. E. and Li, W.
Applied Nonlinear Control.
Upper Saddle River, NJ: Prentice-Hall, 1991.

[16] Kendi, T. A. and Doyle, F. J.
An anti-windup scheme for multivariable nonlinear systems.
Journal of Practice and Control, **7**, 5 (1997), 329–343.

[17] Boskovic, J. D., Li, S. M., and Mehra, R. K.
Robust tracking control design for spacecraft under control input saturation.
Journal of Guidance, Control and Dynamics, **27**, 4 (July–Aug. 2004), 627–633.

[18] Bang, H., Tahk, M. J., and Choi, H. D.
Large angle attitude control of spacecraft with actuator saturation.
Control Engineering Practice, **11** (2003), 989–997.

[19] Tandale, M. D., Subbarao, K., and Valasek, J.
Adaptive dynamic inversion control with actuator saturation constraints applied to tracking spacecraft maneuvers.
Journal of the Astronautical Sciences, **52**, 4 (2005), 517–530.

Maryam Malekzadeh received the B.S. degree (2002) in mechanical engineering from Sharif University of Technology, Tehran, Iran, the M.Sc. (2004) and Ph.D. (2010) degrees in aerospace engineering from Amirkabir University of Technology, Tehran, Iran.

Her main research interests are in stability and control of nonlinear systems especially as applied to aerospace vehicle.

Abolghasem Naghash received his B.Sc. degree in mechanical engineering from Sharif University of Technology in Iran in 1987. He received his M.S. and Ph.D. degrees in 1991 and 1995, respectively from University of Minnesota, Minneapolis, in aerospace engineering.

Since 1995 he has been a faculty member of the Aerospace Engineering Department of Amirkabir University of Technology, Tehran, Iran.

Dr. Naghash is the author of several conference and journal papers in the area of aerospace vehicles, dynamics, and control.

Heidar A. Talebi (M'02—SM'08) received the B.S. degree in electronics from Ferdowsi University of Mashhad, Mashhad, Iran, in 1988, the M.Sc. degree (with first-class honors) in electronics from Tarbiat Modarres University, Tehran, Iran, in 1991, and the Ph.D. degree in electrical and computer engineering from Concordia University, Montreal, QC, Canada, in 1997.

He was a Postdoctoral Fellow and a Research Fellow at Concordia University and the University of Western Ontario. In 1999, he joined Amirkabir University of Technology, Tehran, Iran, where he was the Head of the Control Systems Group from 2002 to 2004 and the deputy chair in research from 2008 to 2009. He is currently an associate professor and the deputy chair in education. His current research interests include control, robotics, fault diagnosis and recovery, intelligent systems, adaptive control, nonlinear control, and real-time systems.